British Journal of Pharmacology

DOI:10.1111/j.1476-5381.2010.01073.x
www.brjpharmacol.org

RESEARCH PAPER

Disulphide trapping of the $GABA_A$ receptor reveals the importance of the coupling interface in the action of benzodiazepines

Susan M. Hanson* and Cynthia Czajkowski

Department of Physiology, University of Wisconsin-Madison, Madison, WI, USA

Correspondence
Cynthia Czajkowski, Department of Physiology, University of Wisconsin-Madison, 601 Science Drive, Madison, WI 53711, USA.
E-mail: czajkowski@physiology.wisc.edu

*Present address: Carroll University, 100 N East Avenue, Waukesha, WI 53186, USA.

Keywords
GABA; GABA receptor; benzodiazepine; flurazepam; zolpidem; allosteric modulation; disulphide bond; disulphide trapping; crosslinking

Received
11 June 2010
Revised
15 September 2010
Accepted
23 September 2010

BACKGROUND AND SIGNIFICANCE

Although the functional effects of benzodiazepines (BZDs) on $GABA_A$ receptors have been well characterized, the structural mechanism by which these modulators alter activation of the receptor by GABA is still undefined.

EXPERIMENTAL APPROACH

We used disulphide trapping between engineered cysteines to probe BZD-induced conformational changes within the γ_2 subunit and at the α_1/γ_2 coupling interface (Loops 2, 7 and 9) of $\alpha_1\beta_2\gamma_2$ $GABA_A$ receptors.

KEY RESULTS

Crosslinking γ_2Loop 9 to γ_2 β-strand 9 (via γ_2S195C/F203C and γ_2S187C/L206C) significantly decreased maximum potentiation by flurazepam, suggesting that modulation of GABA-induced current (I_{GABA}) by flurazepam involves movements of γ_2Loop 9 relative to γ_2 β-strand 9. In contrast, tethering γ_2 β-strand 9 to the γ_2 pre-M1 region (via γ_2S202C/S230C) significantly enhanced potentiation by both flurazepam and zolpidem, indicating γ_2S202C/S230C trapped the receptor in a more favourable conformation for positive modulation by BZDs. Intersubunit disulphide bonds formed at the α/γ coupling interface between α_1Loop 2 and γ_2Loop 9 (α_1D56C/γ_2L198C) prevented flurazepam and zolpidem from efficiently modulating I_{GABA}. Disulphide trapping α_1Loop 2 (α_1D56C) to γ_2 β-strand 1 (γ_2P64C) decreased maximal I_{GABA} as well as flurazepam potentiation. None of the disulphide bonds affected the ability of the negative modulator, 3-carbomethoxy-4-ethyl-6,7-dimethoxy-β-carboline (DMCM), to inhibit I_{GABA}.

CONCLUSIONS AND IMPLICATIONS

Positive modulation of $GABA_A$ receptors by BZDs requires reorganization of the loops in the α_1/γ_2 coupling interface. BZD-induced movements at the α/γ coupling interface likely synergize with rearrangements induced by GABA binding at the β/α subunit interfaces to enhance channel activation by GABA.

Abbreviations

BZD, benzodiazepine; DMCM, 3-carbomethoxy-4-ethyl-6,7-dimethoxy-β-carboline; DTT, dithiothreitol; WT, wild-type

Introduction

$GABA_A$ receptors are allosteric proteins that couple GABA binding to the opening of a chloride-conducting channel. They are members of the pentameric family of ligand-gated ion channels that also includes glycine, 5-HT type 3 and nicotinic acetylcholine receptors (receptor and channel nomenclature follows Alexander *et al.*, 2009). $GABA_A$ receptors are comprised of five homologous subunits arranged pseudo-symmetrically around a central transmembrane channel. The majority of $GABA_A$ receptors in the brain consist

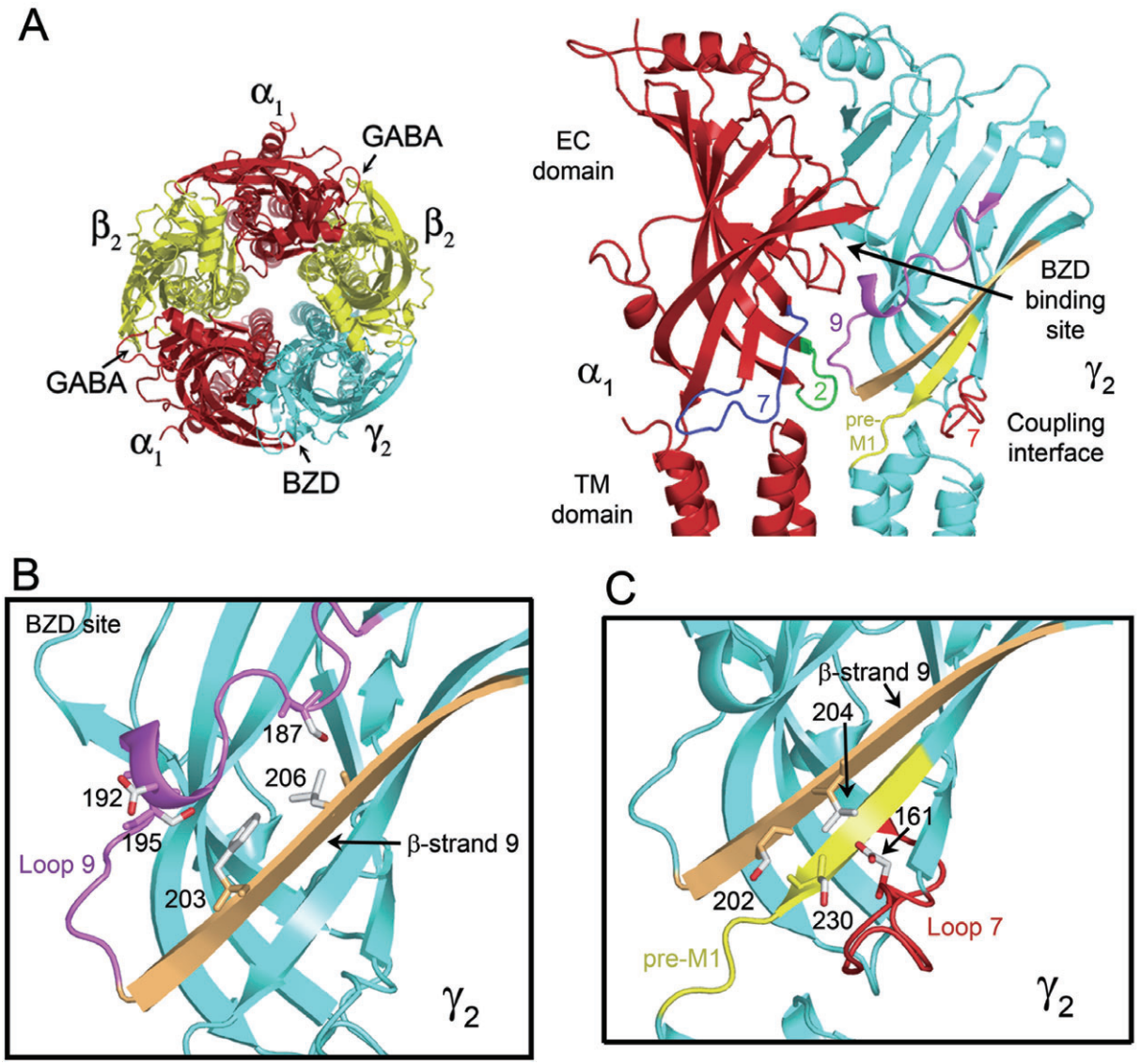

Figure 1

$GABA_A$ receptor structure and the γ_2 subunit coupling interface. (A) *Left*, homology model of the $\alpha_1\beta_2\gamma_2$ $GABA_A$ receptor pentamer (Mercado and Czajkowski, 2006) as seen from the extracellular membrane surface. The α_1, β_2 and γ_2 subunits are highlighted in red, yellow and blue respectively. Arrows indicate that GABA binds at the β_2/α_1 interfaces whereas benzodiazepines (BZDs) bind at the α_1/γ_2 interface of the receptor. *Right*, side view of the α_1 (red) and γ_2 (blue) extracellular domains. Note most of the transmembrane region has been removed for clarity. The general location of the BZD binding site is indicated by an arrow. Several loops at the coupling interface are highlighted as follows: γ_2Loop 9, purple; $\gamma_2$pre-M1, yellow; γ_2Loop 7, red; α_1Loop2, green; α_1Loop7, blue. (B) and (C) close-up view of the γ_2 subunit coupling interface showing residues mutated to cysteine in stick representation. Loops are coloured as indicated above. β-strand 9 is highlighted in orange.

of two α, two β and one γ subunit arranged in a clockwise orientation αβαβγ when viewed from the extracellular side of the membrane (Baumann *et al.*, 2002) (Figure 1A). Each subunit has a large N-terminal extracellular domain, a similarly sized C-terminal domain consisting of four α-helical membrane-spanning segments (M1-M4), and a large cytoplasmic loop between M3 and M4. The channel is formed by residues from the M2 helices of each of the subunits (Xu and Akabas, 1996). Each receptor has two GABA binding sites located in the extracellular domain at the β/α subunit interfaces (reviewed in (Akabas, 2004)(Figure 1A). In each subunit, flexible loops (Loop 2, Loop 7, Loop 9, pre-M1 and the M2-M3 linker) lie at the interface between the extracellular domain and the transmembrane domain (the 'coupling interface') (Figure 1A), which functionally couple the binding domain to the channel domain for all members of the pentameric family of ligand-gated ion channel receptor family (see Sine and Engel, 2006).

$GABA_A$ receptor function is modulated by a number of clinically important drugs including the benzodiazepines (BZDs), barbiturates, anaesthetics and ethanol. BZDs are widely prescribed drugs and exert their anxiolytic, muscle relaxant, sedative and anti-epileptic actions by binding to $GABA_A$ receptors and allosterically modulating GABA-

induced current (I_{GABA}) responses. The BZD binding site is located extracellularly at the α/γ interface (Figure 1A) at a position homologous to the GABA binding sites at the β/α interfaces (see Sigel, 2002). Many structurally diverse ligands bind to the BZD site, including BZD and non-BZD agonists that potentiate I_{GABA} (positive modulators such as flurazepam and zolpidem), BZD inverse agonists that inhibit I_{GABA} (negative modulators such as DMCM), and BZD antagonists that bind at the BZD site but have no effect on I_{GABA}.

The exact mechanism by which these modulators exert their influence on the $GABA_A$ receptor is still debated. Previous studies have led to different conclusions including; that BZDs alter the conductance of the ion channel (Eghbali *et al.*, 1997); that the rate of desensitization is affected (Mellor and Randall, 1997); that the GABA binding rate (Rogers *et al.*, 1994; Lavoie and Twyman, 1996) or dissociation rate (Mellor and Randall, 1997) is changed, and that the channel closed-to-open gating equilibrium is altered (Downing *et al.*, 2005; Rusch and Forman, 2005; Campo-Soria *et al.*, 2006). Many of the identified BZD binding site residues are in homologous positions to residues on the β and α subunits that participate in GABA binding. These observations suggest that the structural mechanisms that couple BZD binding to receptor modulation may be similar to movements induced by GABA binding to promote channel gating.

The therapeutic value of BZDs depends upon how they modulate I_{GABA}, hence elucidating the structural elements that underlie BZD efficacy is crucial. Previously, using γ_2/α_1 chimeric subunits, we identified residues located in the γ_2 subunit pre-M1 region, extracellular end of M2 and M2-M3 linker that were required for modulation of I_{GABA} by BZD agonists (Boileau *et al.*, 1998; Boileau and Czajkowski, 1999). We also recently identified γ_2Loop F/9 as a key element in an allosteric pathway that relays positive BZD modulator-induced structural changes at the BZD binding site to the coupling interface (Hanson and Czajkowski, 2008). Here, we tested the hypothesis that the coupling of BZD binding to modulation of I_{GABA} is mediated, at least in part, via the coupling interfaces in the α_1 and γ_2 subunits. We introduced targeted pairs of cysteines to disulphide trap and constrain movement in the γ_2 subunit and between the α_1 and γ_2 subunits. Both intrasubunit and intersubunit disulphide crosslinking at the α_1/γ_2 coupling interface altered modulation by positive but not negative BZD modulators. Moreover, constraining movement of α_1Loop 2 at the α_1/γ_2 coupling interface significantly impaired GABA-activated channel gating as well as BZD potentiation of I_{GABA}. These results demonstrate that GABA-induced channel activation and positive modulation by BZD-site agonists require reorganization of the loops in the α_1/γ_2 coupling interface.

Methods

Site-directed mutagenesis

Rat cDNA encoding α_1, β_2 and γ_{2L} $GABA_A$ receptor subunits in the pUNIV vector (Venkatachalan *et al.*, 2007) were used for all molecular cloning and functional studies. All γ_{2L} and α_1 cysteine mutants were made by recombinant PCR and verified by double-stranded DNA sequencing.

Expression in Xenopus laevis *oocytes*

All animal care and experimental protocols were in accordance with the guidelines of the National Institutes of Health and were approved by the Animal and Use Committee of the University of Wisconsin. *X. laevis* were housed in fully accredited University of Wisconsin Animal Care facilities. Oocytes were harvested and prepared as described previously (Boileau *et al.*, 1998). Capped cRNA was transcribed *in vitro* from *NotI*-linearized cDNA using the mMessage mMachine T7 kit (Ambion, Austin, TX, USA). Oocytes were injected within 24 h of treatment with 27 nL (1–15 pg·nL^{-1} per subunit) in the ratio 1:1:10 (α:β:γ) (Boileau *et al.*, 2002) and stored at 16°C in ND96 buffer [(in mM) 96 NaCl, 2 KCl, 1 $MgCl_2$, 1.8 $CaCl_2$, 5 HEPES, pH 7.2] supplemented with 100 μg·mL^{-1} gentamycin and 100 μg·mL^{-1} BSA until used for electrophysiological recordings.

Two-electrode voltage clamp

Oocytes were perfused continuously (5 mL·min^{-1}) with ND96 while held under two-electrode voltage clamp at –80 mV in a bath volume of 200 μL. Borosilicate glass electrodes (0.4–1.0 MΩ) (Warner Instruments, Hamden, CT, USA) used for recordings were filled with 3 M KCl. Electrophysiological data were collected using GeneClamp 500 (Axon Instruments, Foster City, CA, USA) interfaced to a computer with a Digidata 1200 A/D device (Axon Instruments), and were recorded using the Whole Cell Program, v.3.8.9 (kindly provided by J. Dempster, University of Strathclyde, Glasgow, UK).

Concentration–response analysis

For the single-cysteine mutants, six to eight concentrations of GABA were used for each determination of GABA EC_{50}. Each response was scaled to a low, non-desensitizing concentration of GABA ($EC_{1\text{-}5}$) applied just before the test concentration to correct for any drift in I_{GABA} responsiveness over the course of the experiment. All concentration–response data were fitted to the following equation: $I = I_{max}/(1 + (EC_{50}/[A])^n)$, where I is the peak response to a given drug concentration, I_{max} is the maximum amplitude of current, EC_{50} is the drug concentration that produces a half-maximal response, $[A]$ is drug concentration, and n is the Hill coefficient using Prism v.5.02 (GraphPad, San Diego, CA, USA). For all mutant and wild-type (WT) receptors, the maximal current responses were ≥5 μA and were achieved with 10 mM GABA. For double cysteine mutant receptors, GABA EC_{50} was estimated by examining the ratio of response to a sub-maximal concentration of GABA (1–50 μM) ($GABA_{sub\text{-}max}$) versus 10 mM GABA ($GABA_{max}$). Using a standard Hill equation to model the GABA dose–responses and the determined ($GABA_{sub\text{-}max}$)/($GABA_{max}$) current ratio, we calculated GABA EC_{50} values (Boileau and Czajkowski, 1999). This measurement also required using an estimated n_H value, which was based on the experimentally determined Hill coefficients of the single-mutant receptors, all of which (except one: D56C) fell within a very tight range: 1.2–1.5. Given this range, the GABA EC_{50} value using the lowest measured n_H for either single mutant and the highest measured n_H for either single mutant fell within 10% of each other and the average of these values is the reported EC_{50}. The reported EC_{50} values for these mutants are the average of estimates performed on multiple oocytes.

Benzodiazepine modulation was defined as: [($I_{GABA+BZD}$/I_{GABA}) – 1], where $I_{GABA+BZD}$ is the current response in the presence of GABA and BZD, and I_{GABA} is the current evoked by GABA alone. BZD modulation was measured at GABA EC_5 for each mutant. For each oocyte, GABA EC_5 was determined prior to each BZD modulation experiment as described above using a ($GABA_{sub-max}$)/($GABA_{max}$) current ratio and a standard Hill equation to model the GABA dose-responses.

Dithiothreitol (DTT) and H_2O_2 treatment

Dithiothreitol (Fisher) was dissolved in water to make a 1 M stock solution and stored at –20°C. DTT and hydrogen peroxide (H_2O_2) (3%; Fisher) were diluted in ND96 buffer to final concentrations of 10 mM and 0.3%, respectively, before each experiment.

Before application of DTT or H_2O_2, oocytes were stabilized by applying GABA (EC_{50}) at 3 min intervals until the I_{GABA} peak current amplitude varied by <5% (generally 2–3 pulses). After achieving current stability, 10 mM DTT was applied for 2 min, followed by a 2 min wash period. GABA (EC_{50}) was applied again. In each case, current amplitude remained stable with multiple GABA applications. Oocytes were then treated with 0.3% H_2O_2 for 2 min, followed by a 2 min wash and GABA (EC_{50}) test pulses. A second treatment of 10 mM DTT for 2 min, followed by GABA (EC_{50}) application was used to assess the reversibility of the H_2O_2 effect.

Dithiothreitol and H_2O_2 effects on BZD modulation of I_{GABA} was measured similarly. After stabilization of I_{GABA} (EC_5) current, maximum BZD modulation was measured. This was followed by an 8 min (flurazepam) or 10 min (zolpidem) wash before the 2 min application of DTT or H_2O_2, wash and subsequent measurement of BZD modulation of I_{GABA}.

Methanethiosulfonate (MTS) modification

Three derivatives of MTS were used to covalently modify the introduced cysteines: MTS-ethylammonium biotin (MTSEA-Biotin), MTS-ethyltrimethylammonium (MTSET) and N-biotinylcaproylaminoethyl-MTS (MTSEA-Biotin CAP) (Toronto Research Chemicals, Toronto, Ontario, Canada). All GABA responses were stabilized by applying GABA (EC_{50}) at 3 min intervals until the peak currents varied by <5%. After achieving current stability, 10 mM DTT was applied for 2 min, followed by a 2 min wash period. I_{GABA} was measured again at 3 min intervals until stable. Oocytes were then treated with 2 mM MTS for 2 min, washed for 2 min, and I_{GABA} was remeasured. The effect of the MTS reagent was calculated as: [(($I_{GABAafter}$ /$I_{GABAbefore}$) − 1) × 100].

Structural modelling

A homology model, based on the crystal structure of the *Lymnaea* acetylcholine-binding protein (Brejc *et al*. 2001) for the extracellular domain, and the 4 Å structure of the *Torpedo* nicotine acetylcholine receptor (Miyazawa *et al*. 2003) for the transmembrane domain, was constructed for the rat $GABA_A$ receptor as described (Mercado and Czajkowski, 2006). In brief, amino acid sequences of the $GABA_A$ receptor were aligned and threaded onto the parent structures, then energy minimized with SYBYL (Tripos Inc. St. Louis, MO, USA). The two domains were then physically docked and again energy-minimized in SYBYL.

The $GABA_A$ receptor model images were developed using PyMOL (DeLano Scientific, Palo Alto, CA, USA).

Statistical analysis

All data were obtained from at least three different oocytes from at least two different frogs. The data were analysed by one-way ANOVA with Dunnett's post-test for significance of differences using Prism v.5.02 (GraphPad, San Diego, CA, USA).

Materials

We used the BZD-site agonists, flurazepam (Research Biochemicals, Natick, MA, USA) and zolpidem (Sigma-Aldrich, St. Louis, MO, USA) and the BZD inverse agonist 3-carbomethoxy-4-ethyl-6,7-dimethoxy-β-carboline (DMCM) (Sigma-Aldrich). Stock solutions of flurazepam and zolpidem (10 mM; H_2O) and DMCM (10 mM; DMSO) were stored at –20°C and diluted in ND96 buffer prior to use. The concentrations of flurazepam and zolpidem used for maximum modulation of I_{GABA} were independently determined for wild type and each mutant receptor to be 10 μM flurazepam and 10 μM zolpidem. Concentrations below this level (1 and 3 μM) did not evoke maximum potentiation and concentrations above this level (30 μM) did not increase potentiation beyond that achieved at 10 μM for any mutant.

Results

Disulphide trapping γ_2Loop 9 to γ_2 β-strand 9 reduces flurazepam potentiation of I_{GABA}

In order to test the hypothesis that binding of positive BZD modulators induces movement of γ_2Loop 9 towards β-strand 9 and the membrane (Figure 1), we engineered pairs of cysteines in γ_2Loop 9 and γ_2 β-strand 9 with the idea that a disulphide bond would constrain movement and alter BZD modulation. Residues that possess a C_β-C_β distance between 4 and 8 Å are ideal candidates for disulphide trapping. Disulphide bond formation becomes less likely as the C_β-C_β distance exceeds 12 Å (Careaga and Falke, 1992). Using a structural homology model of the $GABA_AR$ (Mercado and Czajkowski, 2006), we chose three pairs of residues in Loop 9 and β-strand 9: γ_2S187C/L206C and γ_2S195C/F203C, with C_β-C_β distances of ~ 5 Å each, and γ_2D192C/L206C (C_β-C_β ~ 13 Å) to serve as a negative control (Figure 1B). The five single-cysteine mutant γ_2 subunits as well as the three double mutant γ_2 subunits were co-expressed with WT α_1 and β_2 subunits in *Xenopus* oocytes, and characterized using two-electrode voltage clamp.

All of the mutant subunits assembled into $GABA_A$ receptors that responded to GABA. Only three out of eight mutations (γ_2F203C, γ_2S187C/L206C and γ_2S195C/F203C) significantly decreased GABA EC_{50} values, and these were reduced <3.5-fold compared with WT $\alpha_1\beta_2\gamma_2$ receptors (GABA EC_{50} = 29.6 ± 4.0 μM; Table 1), indicating that the cysteine substitutions were tolerated. Maximal flurazepam (10 μM) potentiation of GABA EC_5 currents was unaltered for the single-cysteine mutant receptors and $\alpha_1\beta_2\gamma_2$D192C/L206C as compared with WT receptors (Table 1, Figure 2). In contrast, flurazepam potentiation was significantly decreased for

Table 1

Summary of GABA, flurazepam, and zolpidem data from wild-type (WT) and γ_2 cysteine mutant receptors used for *intra*subunit crosslinking

Mutant position	Receptor	GABA EC_{50} (μM)	n_H	*n*	Flurazepam Maximum potentiation	*n*	Zolpidem Maximum potentiation	*n*
	αβγ	29.6 ± 4.0	1.2 ± 0.1	6	2.76 ± 0.27	8	4.74 ± 0.50	5
Loop 9	αβγS187C	21.6 ± 3.5[a]	1.6 ± 0.1	3	2.72 ± 0.34	3	4.94 ± 0.39	3
Loop 9	αβγD192C	17.3 ± 3.5[a]	1.5 ± 0.2	3	2.19 ± 0.15	3	4.12 ± 0.26	3
Loop 9	αβγS195C	29.6 ± 2.1[a]	1.3 ± 0.1	3	2.54 ± 0.19	5	5.03 ± 0.33	3
β-strand 9	αβγF203C	8.7 ± 1.8**	1.3 ± 0.2	3	2.42 ± 0.26	3	4.52 ± 0.29	3
β-strand 9	αβγL206C	21.2 ± 1.4	1.3 ± 0.2	3	2.71 ± 0.36	3	3.94 ± 0.25	3
9/β-strand 9	αβγS187C/L206C	16.2 ± 4.3*[b]	ND	12	0.76 ± 0.15**	5	3.99 ± 0.25	3
9/β-strand 9	αβγS195C/F203C	8.4 ± 2.7**[b]	ND	12	1.44 ± 0.13**	3	4.44 ± 0.57	3
9/β-strand 9	αβγD192C/L206C	19.3 ± 2.8[b]	ND	4	2.90 ± 0.08	3	5.22 ± 0.34	5
Loop 7	αβγD161C	12.4 ± 3.9**	1.2 ± 0.2	3	4.30 ± 0.61**	4	6.56 ± 0.45**	3
β-strand 9	αβγS202C	23.2 ± 1.0	1.2 ± 0.1	3	2.55 ± 0.15	4	4.71 ± 0.42	3
β-strand 9	αβγV204C	26.5 ± 4.7	1.2 ± 0.1	3	2.45 ± 0.39	4	4.87 ± 0.21	3
pre-M1	αβγS230C	25.6 ± 3.9	1.3 ± 0.1	3	2.84 ± 0.15	4	4.82 ± 0.18	3
7/β-strand 9	αβγD161C/V204C	3.8 ± 1.8**[b]	ND	5	2.21 ± 0.50	5	4.21 ± 0.20	3
β-strand 9/pre-M1	αβγS202C/S230C	33.3 ± 7.0[b]	ND	8	6.23 ± 0.76**	5	7.63 ± 0.81**	3

[a]Hanson and Czajkowski, 2008.
[b]GABA EC_{50} estimated as described in the Methods.
GABA EC_{50} values were derived by non-linear regression of the concentration-response data as described in the Methods. Flurazepam and zolpidem potentiation of $I_{GABA\ (EC5)}$ was calculated as: [($I_{GABA+BZD}/I_{GABA}$) − 1]. Maximum potentiation values were established for each mutant receptor. The values reported are in the presence of 10 μM flurazepam and 10 μM zolpidem. Data represent mean ± SD from *n* experiments. n_H, calculated Hill coefficient. Values significantly different from WT receptors are indicated (*$P < 0.05$, **$P < 0.01$). The loop or β-strand where the cysteine mutation is located is indicated in the leftmost column.
ND, not determined.

$\alpha_1\beta_2\gamma_2$S187C/L206C and $\alpha_1\beta_2\gamma_2$S195C/F203C receptors by 3.6- and 1.9-fold, respectively (Table 1, Figure 2), suggesting that disulphide bonds between these pairs of cysteines may be the underlying cause for the reduced potentiation.

Initially, we assayed for disulphide bonds by measuring the effects of 10 mM DTT (a reducing agent) and 0.3% H_2O_2 (an oxidizing agent) on BZD modulation of I_{GABA}. DTT and H_2O_2 had no effect on flurazepam potentiation of I_{GABA} for WT receptors (Figures 2 and S1). If disulphide bonds were responsible for the decreases in maximum flurazepam potentiation measured for γ_2S187C/L206C and γ_2S195C/F203C mutant receptors, one might expect DTT would restore flurazepam potentiation. Surprisingly, application of DTT or H_2O_2 had no effect on flurazepam potentiation or I_{GABA} responses for the three double cysteine mutant receptors (Figures 2, S1, and data not shown). Increasing the concentration of DTT, time of DTT application, or treatment with another reducing agent, Tris(2-carboxyethyl)phosphine, also had no effect on flurazepam potentiation or I_{GABA} responses for the three double cysteine mutant receptors (data not shown), suggesting that these pairs of cysteines may not be disulphide-linked. Non-reducible disulphide bonds between engineered cysteines have been reported in the $GABA_A$ receptor (Horenstein *et al.*, 2001) and between native cysteines in other proteins (Shelness and Thornburg, 1996; Negroiu *et al.*, 2000). Disulphide reduction by DTT requires access to the disulphide bond at the appropriate orientation. Thus, it is possible that the introduced cysteine pairs formed disulphides that were resistant to reduction by DTT.

In order to help distinguish between free and disulphide-linked cysteines, we examined if the introduced single cysteines and cysteine pairs were accessible to modification by sulphydryl-specific MTS reagents. MTS reagents preferentially modify water-accessible ionized cysteine residues (Karlin and Akabas, 1998). We reasoned that if the single engineered cysteines were modified by MTS reagents but the cysteine pairs were not, then this would provide evidence that the cysteine pairs were participating in a disulphide bond. Similar approaches have been used successfully by Bali *et al.* (2009) to detect whether two cysteines participate in a disulphide bond in the $GABA_A$ receptor transmembrane domain and in voltage-gated K^+channels to detect free versus disulphide-bonded cysteine residues (Lu and Deutsch, 2001; Kosolapov and Deutsch, 2003).

The single- and double-cysteine mutant receptors were pretreated with DTT and then we measured I_{GABA} (EC_{50}) and/or flurazepam potentiation of I_{GABA} before and after exposure to MTSET, MTSEA-Biotin and MTSEA-Biotin CAP. These reagents have no functional effects on WT $GABA_A$ receptors (Figure 3, bar graphs and see Hanson and Czajkowski, 2008). Thus, any changes measured in I_{GABA} or flurazepam potentiation of I_{GABA} following MTS exposure indicate that the introduced cysteines were modified. The MTS reagents had no significant effects on I_{GABA} or flurazepam potentiation of I_{GABA}

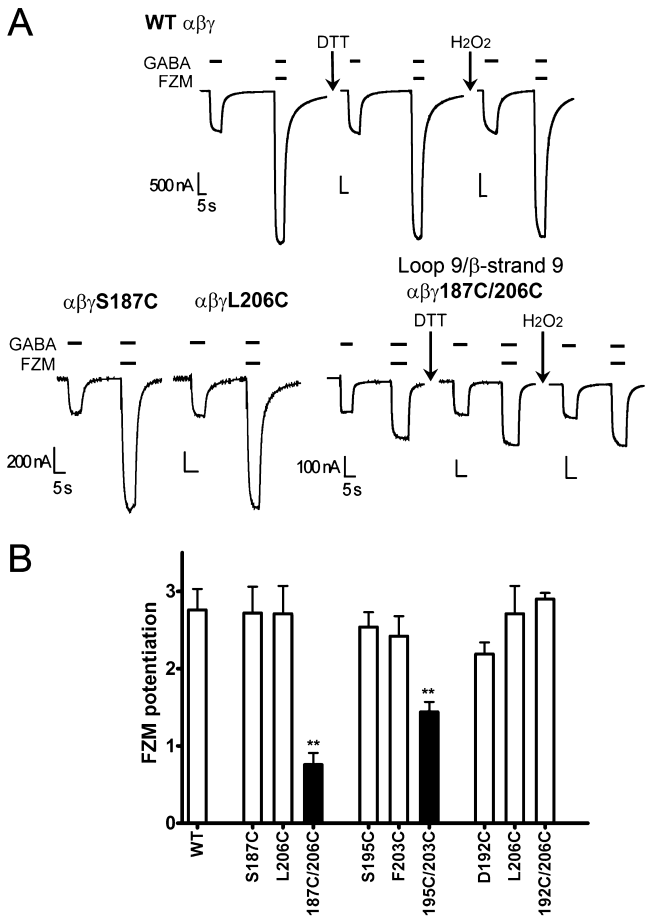

Figure 2

Flurazepam potentiation of I_{GABA} is significantly reduced for $\alpha_1\beta_2\gamma_2$S187C/L206C and $\alpha_1\beta_2\gamma_2$S195C/F203C receptors. Potentiation of GABA EC_5 current by 10 μM flurazepam (FZM) from oocytes injected with wide-type (WT) or mutant receptors. (A) Representative current traces from WT and $\alpha_1\beta_2\gamma_2$S187C/L206C mutant receptors. In order to easily see changes in potentiation, traces are scaled so that the GABA EC_5 current amplitude is the same for each receptor and condition. DTT and H_2O_2 treatment of WT and double cysteine mutant receptors was performed as described in the Methods. Current responses for $\alpha_1\beta_2\gamma_2$S195C/F203C mutant receptors were similar to $\alpha_1\beta_2\gamma_2$S187C/L206C receptors for each condition. Potentiation of GABA current was calculated as [($I_{GABA+FZM}/I_{GABA}$) – 1] and is graphed in (B) and reported in Table 1. (B) Potentiation of I_{GABA} by flurazepam for WT and γ_2-mutant receptors. Black bars indicate mutants in which the change in potentiation was significantly different from WT receptors and the corresponding single-cysteine mutants (**$P < 0.01$). Data represent mean ± SD from at least three separate experiments. In each case, DTT and H_2O_2 treatment of the WT and double cysteine mutant receptors had no significant effects on flurazepam potentiation of I_{GABA}.

for $\alpha_1\beta_2\gamma_2$D192C and $\alpha_1\beta_2\gamma_2$L206C receptors (data not shown) indicating that these introduced cysteines were not accessible to MTS modification or their modification had no functional effect. MTSEA-Biotin CAP significantly increased I_{GABA} in $\alpha_1\beta_2\gamma_2$S187C receptors and MTSEA-Biotin significantly increased I_{GABA} in $\alpha_1\beta_2\gamma_2$S195C and $\alpha_1\beta_2\gamma_2$F203C receptors (Figure 3). MTSET also significantly increased I_{GABA} in $\alpha_1\beta_2\gamma_2$F203C receptors (39.3 ± 2.5%) (data not shown). These data indicate that in single-cysteine mutant receptors γ_2S187C, γ_2S195C and γ_2F203C are ionized and accessible to modification.

In contrast, receptors containing the double-cysteine mutation, γ_2S187C/L206C, showed no significant changes in I_{GABA} compared with WT $GABA_A$ receptors following treatment with MTSEA-Biotin CAP either without or with DTT pretreatment (Figure 3). The MTSEA-Biotin CAP effects on γ_2S187C/L206C were significantly less than that observed with γ_2S187C (Figure 3) and not statistically different from WT receptors. MTSEA-Biotin and MTSET also had no significant effects on γ_2S195C/F203C receptors compared with WT receptors, in contrast to the increases in I_{GABA} observed for $\alpha_1\beta_2\gamma_2$S195C and $\alpha_1\beta_2\gamma_2$F203C receptors following treatment with the same MTS reagents (Figure 3). The observation that MTS treatment had no significant effects on I_{GABA} when γ_2S187C was paired with γ_2L206C (γ_2S187C/L206C) and when γ_2S195C was paired with γ_2F203C (γ_2S195C/F203C) demonstrates that these cysteines are not free sulphydryls and indicates that the cysteines are disulphide-linked and are unavailable to react with the MTS reagents. While one could argue that introduction of two cysteines induces a conformational change in the receptor that renders both cysteines resistant to MTS modification, which is not observed for the single-cysteine substitutions, this seems highly unlikely. Moreover, while not significant, MTSEA-Biotin CAP modification of receptors containing γ_2S187C/L206C showed a small but consistent increase in I_{GABA} following DTT pretreatment (Figure 3A), suggesting reduction of a resistant disulphide bond.

To determine whether modulation of I_{GABA} by other BZD ligands was also affected by the single- and double-cysteine mutations, we measured maximum potentiation of I_{GABA} by zolpidem, a structurally distinct BZD-site agonist, and inhibition of I_{GABA} by the BZD inverse agonist, DMCM. Interestingly, for all of the above single- and double-cysteine mutant receptors, zolpidem (10 μM) maximally potentiated I_{GABA} to a similar extent as WT receptors (Figure 4, Table 1). In addition, the maximal inhibition of I_{GABA} by 1 μM DMCM was not significantly different for the single- and double-cysteine mutant receptors as compared with WT receptors (DMCM inh = –0.66 ± 0.02) (Figures 4 and S2). The observations that zolpidem potentiation and DMCM inhibition of I_{GABA} were unchanged indicate that γ_2S187C/L206C and γ_2S195C/F203C do not impair γ_2-subunit assembly or incorporation into functional $GABA_A$ receptors. Moreover, these results demonstrate that the effects of the mutations on flurazepam potentiation are not due to changes in GABA EC_{50} values but are specific to flurazepam actions and suggest the coupling of flurazepam binding to potentiation involves unique movements of γ_2Loop 9 relative to γ_2 β-strand 9.

Disulphide trapping γ_2 β-strand 9 to γ_2 pre-M1 increases flurazepam and zolpidem potentiation of I_{GABA}

Two flexible loops, the pre-M1 region and Loop 7, lie between γ_2Loop 9, β-strand 9 and the transmembrane domain (Figure 1C). To test the hypothesis that movements in γ_2Loop 9 and γ_2 β-strand 9 initiated by flurazepam binding get transduced to the transmembrane domain via γ_2 pre-M1 we

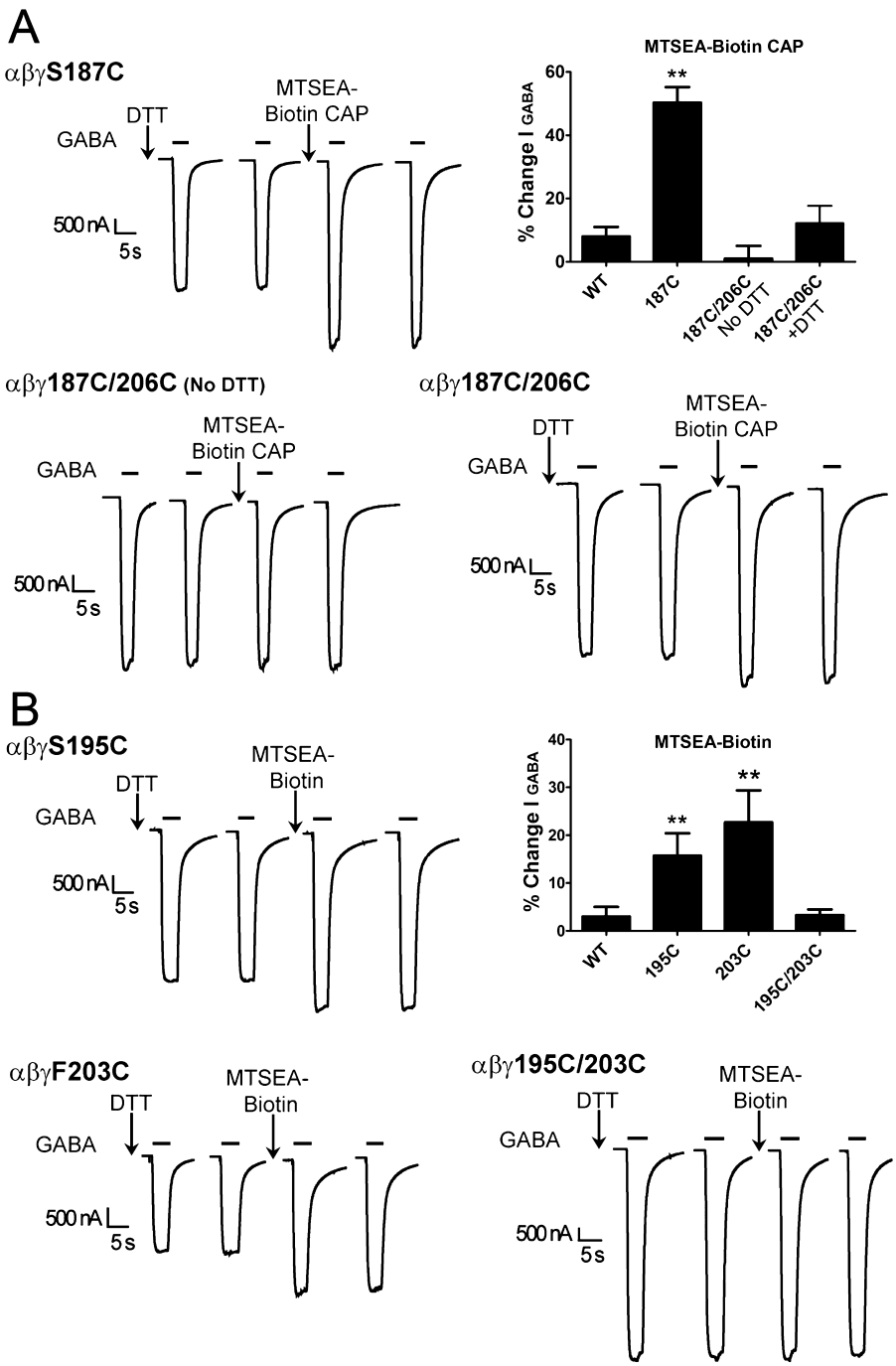

Figure 3

Methanethiosulfonate (MTS) modifies single-cysteine mutant receptors but not double cysteine mutant $\alpha_1\beta_2\gamma_2$S187C/L206C or $\alpha_1\beta_2\gamma_2$S195C/F203C receptors. (A) Representative GABA EC_{50} currents from oocytes expressing $\alpha_1\beta_2\gamma_2$S187C and $\alpha_1\beta_2\gamma_2$S187C/L206C receptors before and after treatment with 2 mM N-biotinylcaproylaminoethyl-MTS (MTSEA-Biotin CAP). Receptors were pre-treated with 10 mM dithiothreitol (DTT) for 2 min, except where noted. Changes in I_{GABA} following treatment with MTSEA-Biotin CAP are summarized in the bar graph and were calculated as: [(($I_{GABAafter}$ /$I_{GABAbefore}$) − 1) × 100]. Note that MTS treatment of $\alpha_1\beta_2\gamma_2$S187C receptors significantly increases I_{GABA} compared to wide-type (WT) receptors (**P < 0.01), whereas the change in I_{GABA} following MTS treatment of $\alpha_1\beta_2\gamma_2$S187C/L206C receptors both with and without DTT pretreatment is not statistically different from WT receptors. Data represent mean ± SD from at least three separate experiments. (B) Representative GABA EC_{50} currents from $\alpha_1\beta_2\gamma_2$S195C, $\alpha_1\beta_2\gamma_2$F203C, and $\alpha_1\beta_2\gamma_2$S195C/F203C receptors recorded before and after treatment with 2 mM MTSEA-Biotin. Changes in I_{GABA} following treatment with MTSEA-Biotin are summarized in the bar graph. Note that MTS treatment of single-cysteine mutant receptors significantly increases I_{GABA} compared to WT receptors (**P < 0.01), whereas the change in I_{GABA} following MTS treatment of $\alpha_1\beta_2\gamma_2$S195C/F203C receptors is not significantly different from WT receptors. Data represent mean ± SD from at least three separate experiments.

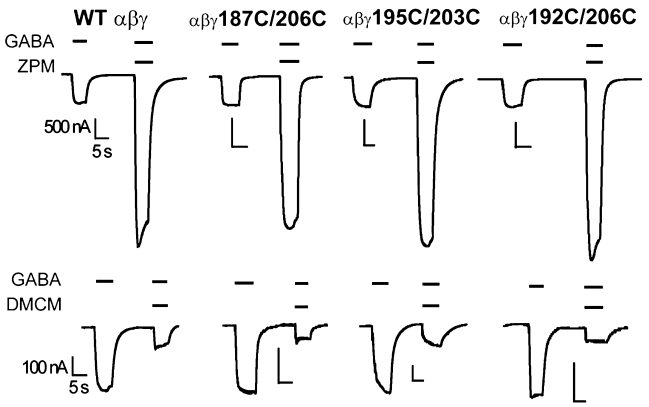

Figure 4

Zolpidem and 3-carbomethoxy-4-ethyl-6,7-dimethoxy-β-carboline (DMCM) modulation of I_{GABA} is unchanged for γ_2Loop 9/β-strand 9 double cysteine mutant receptors. Modulation of GABA EC_5 currents by 10 μM zolpidem (ZPM) (*top*) or 1 μM DMCM (*bottom*) from oocytes expressing wild-type (WT) and mutant receptors. In order to easily see changes in modulation, traces are scaled so that the GABA EC_5 current amplitude is the same for each receptor. Modulation of GABA current was calculated as $[(I_{GABA+BZD}/I_{GABA}) - 1]$. Values for zolpidem potentiation are reported in Table 1. Zolpidem potentiation and DMCM inhibition for the mutant receptors were not significantly different from WT.

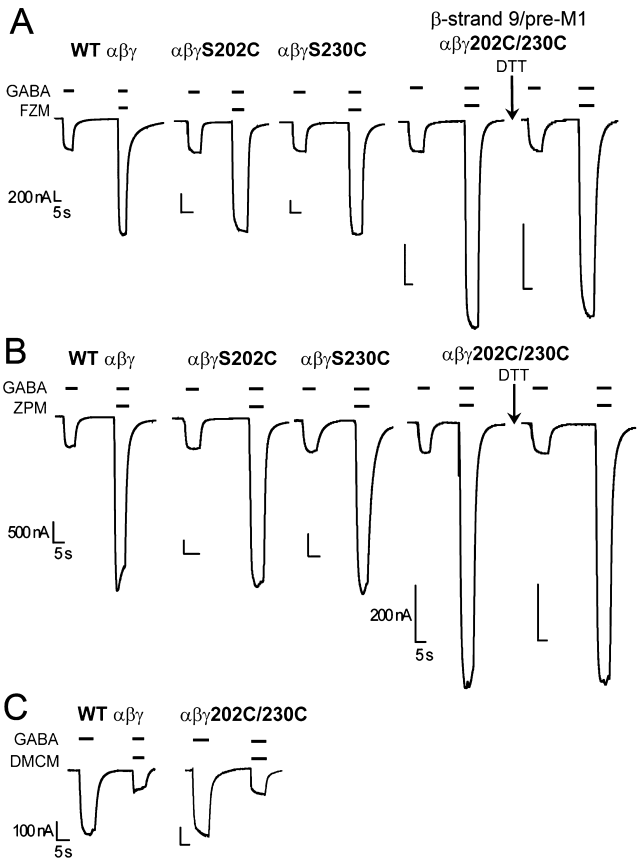

Figure 5

Flurazepam and zolpidem potentiation of I_{GABA} is significantly increased for $\alpha_1\beta_2\gamma_2$S202C/S230C receptors. Modulation of GABA EC_5 currents by 10 μM flurazepam (FZM; A), 10 μM zolpidem (ZPM; B), or 1 μM DMCM (C), from oocytes injected with wild-type (WT) or mutant receptors. In order to easily see changes in potentiation, traces are scaled so that the GABA EC_5 current amplitude is the same for each receptor and condition. Dithiothreitol (DTT) treatment of $\alpha_1\beta_2\gamma_2$S202C/S230C receptors was performed as described in the Methods. Values for flurazepam and zolpidem potentiation are reported in Table 1. For $\alpha_1\beta_2\gamma_2$S202C/S230C receptors, flurazepam and zolpidem potentiation was significantly increased compared to WT and the corresponding single-cysteine mutants, whereas DMCM inhibition was not altered. In each case, DTT and H_2O_2 (not shown) treatment of $\alpha_1\beta_2\gamma_2$S202C/S230C had no significant effect on potentiation.

engineered a pair of cysteines in γ_2 β-strand 9 and γ_2 pre-M1 (γ_2S202C/S230C, C_β-C_β ~ 4 Å), to restrict local movements in this region (Figure 1C).

Mutations in γ_2S202C, γ_2S230C and γ_2S202C/S230C had no effect on GABA EC_{50} values compared with WT receptors (GABA EC_{50} = 30 μM; Table 1). Flurazepam and zolpidem potentiation of I_{GABA} was also unaltered for $\alpha_1\beta_2\gamma_2$S202C and $\alpha_1\beta_2\gamma_2$S230C receptors as compared with WT receptors, whereas flurazepam and zolpidem potentiation of I_{GABA} for the double mutant $\alpha_1\beta_2\gamma_2$S202C/S230C receptor was increased by 2.3- and 1.6-fold respectively (Figure 5, Table 1). None of the mutations significantly affected inhibition of I_{GABA} by DMCM (Figures 5C and S2). Thus, the effects of the γ_2S202C/S230C mutation are specific for modulation by BZD-site agonists.

As observed with $\alpha_1\beta\gamma_2$S187C/L206C and $\alpha_1\beta_2\gamma_2$S195C/F203C receptors, neither DTT nor H_2O_2 had any effect on flurazepam or zolpidem potentiation of I_{GABA} or on I_{GABA} alone for $\alpha_1\beta_2\gamma_2$S202C/S230C receptors (Figure 5 and data not shown). To assess whether γ_2S202C/S230C existed as free or disulphide-linked cysteines, we examined the ability of MTS reagents to modify the introduced single- and double-cysteine residues. MTSET significantly increased I_{GABA} in $\alpha_1\beta_2\gamma_2$S202C and $\alpha_1\beta_2\gamma_2$S230C receptors compared with WT $GABA_A$ receptors (Figure 6). For the double cysteine mutant $\alpha_1\beta_2\gamma_2$S202C/S230C receptor, the effect of MTSET on I_{GABA} (Figure 6) was significantly less than its effects on the two single-cysteine mutants and was not statistically different from WT receptors. These data suggest that γ_2S202C and γ_2S230C, when expressed together, are disulphide-linked and that crosslinking γ_2 β-strand 9 (S202C) to γ_2 pre-M1 (S230C) enhances potentiation of I_{GABA} by flurazepam and zolpidem.

Disulphide trapping γ_2 β-strand 9 to γ_2 Loop 7

To test the hypothesis that movements in γ_2Loop 9 and γ_2 β-strand 9 initiated by flurazepam binding get transduced to the transmembrane domain via γ_2Loop 7, we also engineered a pair of cysteines in this region (γ_2D161C/V204C, C_β-C_β ~ 5 Å) (Figure 1C). Maximum flurazepam and zolpidem potentiation of I_{GABA} was significantly increased for $\alpha_1\beta_2\gamma_2$D161C receptors by 1.6- and 1.4-fold respectively, but was unaltered for $\alpha_1\beta_2\gamma_2$V204C and $\alpha_1\beta_2\gamma_2$D161C/V204C receptors (Table 1). None of the mutations significantly affected inhibition of I_{GABA} by DMCM (Figure S2). Neither DTT nor H_2O_2 had any effect on flurazepam or zolpidem potentiation of I_{GABA} or on

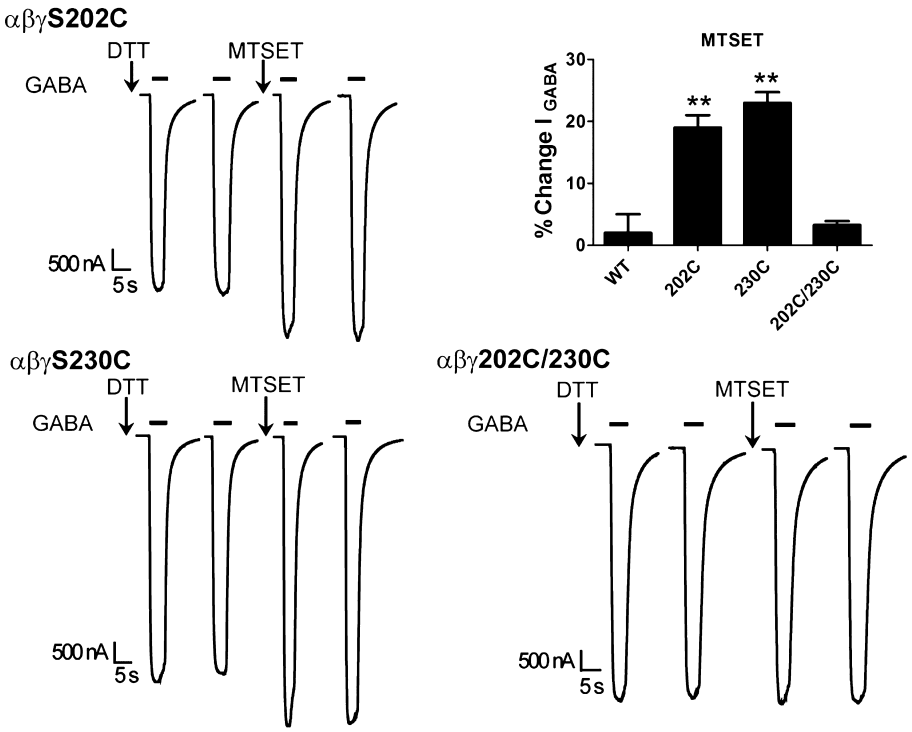

Figure 6

Methanethiosulfonate (MTS) modifies $\alpha_1\beta_2\gamma_2$S202C and $\alpha_1\beta_2\gamma_2$S230C receptors but not $\alpha_1\beta_2\gamma_2$S202C/230C receptors. Representative GABA EC_{50} traces from $\alpha_1\beta_2\gamma_2$S202C, $\alpha_1\beta_2\gamma_2$S230C, and $\alpha_1\beta_2\gamma_2$S202C/230C receptors before and after treatment with 2 mM MTS-ethyltrimethylammonium (MTSET). All receptors were pre-treated with 10 mM dithiothreitol (DTT) for 2 min. Changes in I_{GABA} following treatment with MTSET are summarized in the bar graph and were calculated as: $[((I_{GABAafter} / I_{GABAbefore}) - 1) \times 100]$. Note that MTS treatment of single-cysteine mutant receptors significantly increases I_{GABA} compared to WT receptors (**$P < 0.01$), whereas the change in I_{GABA} following MTS treatment of $\alpha_1\beta_2\gamma_2$S202C/S230C receptors is not significantly different from WT receptors. Data represent mean ± SD from at least three separate experiments.

I_{GABA} alone for $\alpha_1\beta_2\gamma_2$D161C/V204C receptors and none of the MTS reagents had significant effects (<10%) on I_{GABA} for $\alpha_1\beta_2\gamma_2$D161C and $\alpha_1\beta_2\gamma_2$V204C receptors (data not shown). Thus, we could not assess whether a disulphide bond between the two residues had formed.

Intersubunit disulphide trapping at the α_1/γ_2 coupling interface reduces flurazepam potentiation

Recently, we demonstrated that movements in γ_2Loop 9 at the α/γ coupling interface are triggered specifically by positive BZD modulators (Hanson and Czajkowski, 2008). We speculated that γ_2Loop 9 movements are propagated to residues in the adjacent α_1 subunit via α_1Loops 2 and 7 due to their proximity in structural models (Figures 1A and S3). To test this hypothesis, we made seven individual cysteine mutations in γ_2Loop 9 (R194C-Q200C), and combined them with single-cysteine mutations in α_1Loop 2 (D56C, M57C), and α_1Loop 7 (E137C, P139C) to create 15 α/γ double-cysteine mutant receptors in order to probe the proximity and dynamics of these regions (Figure S3). Our model also predicted a close interaction (C_β-C_β 5.8 Å) between α_1Loop 2 (D56) and γ_2 β-strand 1 (P64) and thus, we also examined this double cysteine mutant.

Six out of the 11 single-cysteine mutations significantly decreased flurazepam maximal potentiation of I_{GABA} (α_1M57C, α_1E137C, α_1P139C, γ_2P64C, γ_2R197C, γ_2Q200C) and one mutation, α_1D56C, increased flurazepam potentiation (Tables 2 and S1) indicating that residues distributed throughout the α/γ coupling interface are important for regulating BZD efficacy. Changes in potentiation were not correlated to changes in GABA EC_{50} values. For example, flurazepam potentiation was decreased for α_1M57C, α_1E137C, and γ_2R197C but the GABA EC_{50} values for these mutants was increased, decreased and unchanged, respectively, compared with WT receptors. For four of the double-cysteine mutants (α_1D56C/γ_2R194C, α_1D56C/γ_2S195C, α_1D56C/γ_2W196C, α_1D56C/γ_2Q200C), flurazepam potentiation was in-between that of the two corresponding singles (Figure S1 and Table S1), suggesting a simple additive effect of the mutations. For the other double mutants, flurazepam potentiation was either not statistically different from one of the single-cysteine mutants (α_1D56C/γ_2R197C, α_1D56C/γ_2Y199C, α_1M57C/γ_2Y199C, α_1D56C/γ_2P64C, α_1E137C/γ_2R194C, α_1E137C/γ_2W196C) or it was significantly less than the two singles (α_1D56C/γ_2L198C, α_1M57C/γ_2S195C, α_1M57C/γ_2W196C, α_1M57C/γ_2L198C, α_1M57C/γ_2Q200C, α_1P139C/γ_2L198C), suggesting the cysteines interact and are potentially disulphide-linked (Figure S1 and Table S1).

To probe for potential disulphide bonds, we examined the effects of DTT on flurazepam potentiation of I_{GABA}. Only two out of the 16 double α_1/γ_2 mutant receptors were significantly

Table 2

Summary of GABA, flurazepam, and zolpidem data from wild-type (WT) and α_1/γ_2 cysteine mutant receptors that form *inter*subunit disulphide bonds

Mutant position	Receptor	GABA EC_{50} (μM)	n_H	*n*	Flurazepam Maximum potentiation	*n*	Zolpidem Maximum potentiation	*n*
	αβγ	29.6 ± 4.0	1.2 ± 0.1	6	2.76 ± 0.27	8	4.74 ± 0.50	5
2	αD56Cβγ	123.4 ± 38.2**	0.7 ± 0.1	12	5.65 ± 0.30**	4	6.48 ± 0.70**	4
9	αβγL198C	4.7 ± 0.6**	1.4 ± 0.1	3	2.36 ± 0.06	3	3.67 ± 0.70	3
2/9	αD56Cβγ L198C	17 ± 3*[b]	ND	6	1.33 ± 0.44**	5	1.84 ± 0.44**	3
β-strand 1	αβγP64C	6.6 ± 2.6**	1.5 ± 0.1	12	1.82 ± 0.16**	5	3.05 ± 0.06**	3
2/β-strand 1	αD56Cβγ P64C	56 ± 23[b]	ND	5	1.61 ± 0.36**	4	2.39 ± 0.35**	5

[b]GABA EC_{50} estimated as described in the Methods.
GABA EC_{50} values were derived by non-linear regression of the concentration-response data as described in the Methods. Flurazepam and zolpidem potentiation of $I_{GABA\ (EC5)}$ was calculated as: [$(I_{GABA+BZD}/I_{GABA}) - 1$]. Maximum potentiation values were established for each mutant receptor in the absence of any dithiothreitol treatment. Values reported are in the presence of 10 μM flurazepam and 10 μM zolpidem. Data represent mean ± SD from *n* experiments. n_H, calculated Hill coefficient. Values significantly different from WT receptors are indicated (*$P < 0.05$, **$P < 0.01$). The loop or β-strand where the cysteine mutation is located is indicated in the leftmost column.
ND, not determined.

affected by DTT. DTT significantly increased flurazepam potentiation for α_1D56C$\beta_2\gamma_2$L198C (α_1Loop 2/γ_2Loop 9) and α_1D56C$\beta_2\gamma_2$P64C (α_1Loop 2/γ_2 β-strand 1) receptors (Figure 7A). DTT also significantly increased zolpidem potentiation for α_1D56C$\beta_2\gamma_2$L198C receptors (data not shown). DTT had no effect on WT and the corresponding single-cysteine substitutions (Figure 7B). The DTT-induced increase in flurazepam potentiation was reversed by H_2O_2 and a subsequent application of DTT increased flurazepam potentiation to a similar extent as that measured after the first DTT treatment (Figure 7A). From these results, we infer that disulphide bonds between α_1D56C and γ_2L198C and between α_1D56C and γ_2P64C form spontaneously, which inhibit flurazepam potentiation of I_{GABA}. DMCM inhibition of I_{GABA} was unaffected by the α_1D56C/γ_2L198C or α_1D56C/γ_2P64C mutations (Figures 7C and S2) indicating that the receptors assembled into functional αβγ receptors and that the effects exerted by the single- and double-cysteine mutations on flurazepam and zolpidem potentiation were specific for agonists at the BZD site.

For the rest of the α/γ double-cysteine mutants, DTT and H_2O_2 had no effect on flurazepam potentiation compared with WT receptors (data not shown). It is possible that these cysteines formed non-reducible disulphide bonds. For these mutations, we could not use MTS accessibility to probe whether the cysteines were free or disulphide-linked because one of the engineered cysteine residues is in the α subunit. Because each $GABA_A$ receptor has two α subunits (Figure 1A), even if the introduced cysteine at the α/γ interface was trapped in a disulphide bond, the cysteine at the α/β interface would still be freely accessible to react with MTS, which would complicate the analysis.

Disulphide trapping α_1Loop 2 to γ_2 β-strand 1 inhibits I_{GABA}

We also tested the effect of DTT and H_2O_2 on I_{GABA} (EC_{50}) for the 16 α/γ double-cysteine mutants. Only one double-cysteine mutant, α_1D56C/γ_2P64C (Figure 8A) was significantly affected by DTT, which increased the amplitude of $I_{GABA\text{-}EC50}$ (Figure 8C). H_2O_2 completely reversed this effect, restoring I_{GABA} to its initial level. A second application of DTT increased I_{GABA} again about 50%. DTT had no effect on the corresponding single-cysteine mutants (Figure 8C). We conclude that the effects of DTT and H_2O_2 on I_{GABA} are due to the formation and reduction of a disulphide bond between α_1D56C and γ_2P64C.

The peak amplitudes elicited by a saturating concentration of GABA (10 mM) from oocytes expressing α_1D56C$\beta_2\gamma_2$P64C receptors were relatively small (<5 μA) compared with WT receptors (>15 μA) (Figure 8). To determine whether the increase in I_{GABA} following treatment with DTT was due to a shift in the GABA concentration–response curve and/or changes in maximum current amplitude, we measured I_{GABA} at low and saturating concentrations of GABA to estimate GABA EC_{50} values and to determine maximum current before and after treatment with DTT. We found that DTT had a small effect (<20% change) on the calculated GABA EC_{50} value but that the maximum current amplitude from saturating GABA was significantly increased by DTT (Figure 8B), suggesting that crosslinking α_1Loop 2 (D56C) to γ_2 β-strand 1 (P64C) reduces the efficacy of GABA to activate the channel.

Discussion

Although the functional effects of BZDs have been well characterized, the protein movements underlying BZD modulation of $GABA_A$ receptor current are largely undefined. In a previous study, we demonstrated that potentiation of I_{GABA} by positive BZD modulators initiates distinct movements in γ_2Loop 9 (Hanson and Czajkowski, 2008). Here, we used disulphide trapping to examine how movements in Loop 9 and the nearby α_1/γ_2 coupling interface influence BZD modula-

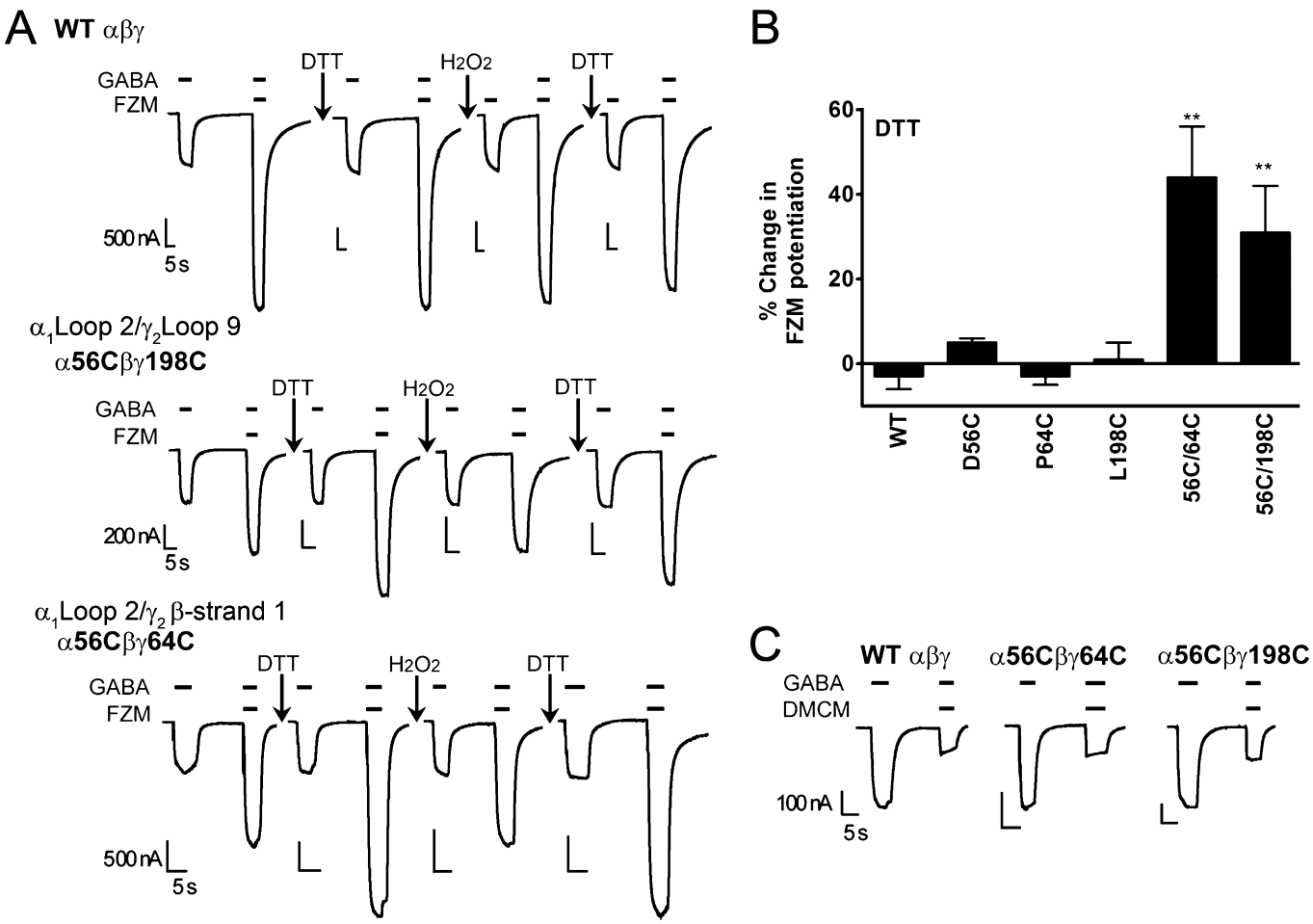

Figure 7

Intersubunit disulphide trapping at the α_1/γ_2 coupling interface reduces flurazepam potentiation of I_{GABA}. Modulation of GABA EC_5 currents by 10 μM flurazepam (FZM; A), or 1 μM 3-carbomethoxy-4-ethyl-6,7-dimethoxy-β-carboline (DMCM) (C), from oocytes injected with wild-type (WT) or mutant receptors. Traces are scaled so that the GABA EC_5 current response is the same for each receptor or condition to compare differences and changes in potentiation. Dithiothreitol (DTT) and H_2O_2 treatment of WT and double cysteine mutant receptors was performed as described in the Methods. Modulation of GABA current was calculated as [$(I_{GABA+BZD}/I_{GABA}) - 1$]. Values for flurazepam potentiation prior to DTT treatment are reported in Table 2. (B) Changes in flurazepam potentiation following treatment with DTT for each receptor and the corresponding single-cysteine mutants are shown in graphical form. The effect of DTT treatment was calculated as: [((flurazepam $potentiation_{after}$/flurazepam $potentiation_{before}$) − 1) × 100]. Note that DTT treatment significantly increased flurazepam potentiation for both α_1D56C$\beta_2\gamma_2$L198C and α_1D56C$\beta_2\gamma_2$P64C receptors compared with WT and the corresponding single-cysteine mutants (**$P < 0.01$). Data represent mean ± SD from at least three separate experiments. (C) Modulation of GABA EC_5 currents by 1 μM DMCM are shown for WT and mutant receptors.

tion of I_{GABA}. Disulphide trapping is a powerful approach for probing protein dynamics of both soluble and membrane-bound proteins in their native environment (Bass *et al.*, 2007) and has been used to study movements in the $GABA_A$ receptor transmembrane segments triggered by both GABA and anaesthetic channel activation (Horenstein *et al.*, 2001; Bera and Akabas, 2005; Horenstein *et al.*, 2005; Jansen and Akabas, 2006; Rosen *et al.*, 2007; Yang *et al.*, 2007; Bali *et al.*, 2009).

Reorganization of the α_1/γ_2 coupling interface accompanies BZD potentiation of I_{GABA}

Based on our electrophysiological assays, disulphide bonds formed between γ_2S187C/L206C, γ_2S195C/F203C, γ_2S202C/S230C, α_1D56C/γ_2P64C and α_1D56C/γ_2L198C (Figures 2,3,5–7). Intrasubunit disulphide trapping γ_2Loop 9 to β-strand 9 in $\alpha_1\beta_2\gamma_2$S187C/L206C and $\alpha_1\beta_2\gamma_2$S195C/F203C receptors significantly reduced maximal flurazepam potentiation (Figures 2 and 9 and Table 1), indicating that modulation of I_{GABA} by flurazepam involves movements of γ_2Loop 9 relative to γ_2 β-strand 9. Because Loop 9 sits near the BZD binding pocket (Figures 1 and 9), tethering Loop 9 to β-strand 9 likely impairs flurazepam potentiation by preventing initial structural rearrangements of Loop 9 induced by flurazepam binding. Interestingly, crosslinking γ_2Loop 9 to β-strand 9 reduced flurazepam potentiation without affecting zolpidem potentiation (Figure 4). These data suggest that zolpidem binding initiates movement in a different part of Loop 9 (i.e. unaffected by crosslinking γ_2S195C/F203C and γ_2S187C/L206C). Consistent with this idea, in a previous study, we showed that mutations in γ_2Loop 9 differentially affect flurazepam and

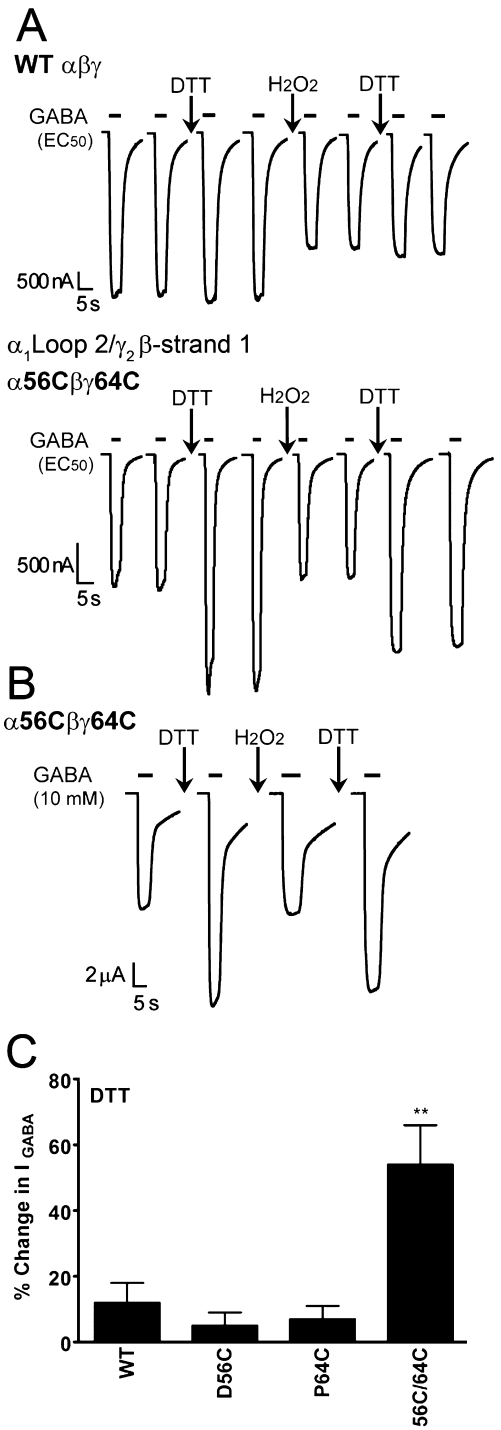

Figure 8

Disulphide trapping α_1Loop 2 to γ_2 β-strand 1 inhibits GABA activation. Representative current traces from wide-type (WT) and α_1D56C$\beta_2\gamma_2$P64C receptors elicited by GABA EC_{50} (A) or 10 mM GABA (~GABA EC_{99}) (B) before and after treatment with dithiothreitol (DTT) and H_2O_2. (C) Changes in GABA EC_{50} current following treatment with DTT are shown. The effect of DTT treatment was calculated as: $[((I_{GABAafter} / I_{GABAbefore}) - 1) \times 100]$. Note that DTT treatment significantly increased I_{GABA} for α_1D56C$\beta_2\gamma_2$P64C receptors compared with WT and the corresponding single-cysteine mutants (**$P < 0.01$). Data represent mean ± SD from at least four separate experiments.

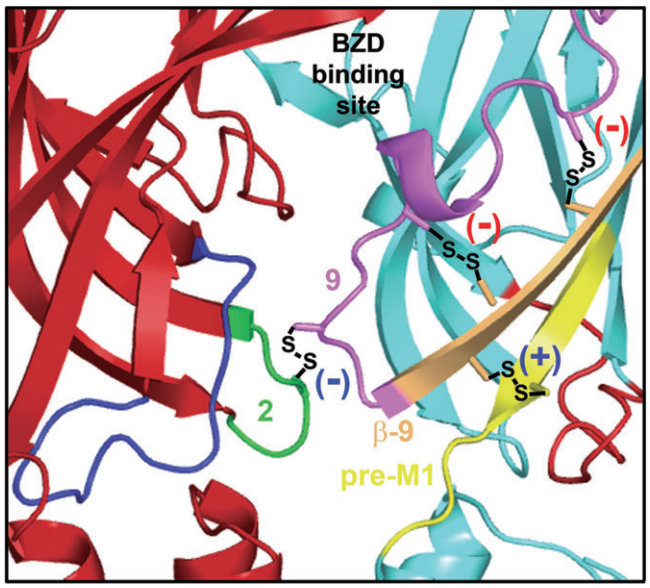

Figure 9

Summary of the effects of disulphide bond formation at the $GABA_AR$ α/γ interface. Homology model of the α_1 (red) and γ_2 (blue) extracellular domains of the $GABA_AR$. The general location of the benzodiazepine (BZD) binding site is indicated. The loops at the coupling interface are highlighted as in Figure 1: γ_2Loop 9, purple; β-strand 9, orange. $\gamma_2$pre-M1, yellow; γ_2Loop 7, red; α_1Loop2, green; α_1Loop7, blue. Disulphide bonds that inhibit (-) and enhance (+) BZD potentiation of I_{GABA} are shown. Bonds that affect both flurazepam and zolpidem potentiation are indicated by a blue (-) (α_1D56C$\beta_2\gamma_2$L198C) or blue (+) (α1$\beta_2\gamma_2$S202C/S230C), while those that only affect flurazepam potentiation are indicated by a red (-)($\alpha_1\beta_2\gamma_2$S187C/L206C and $\alpha_1\beta_2\gamma_2$S195C/F203C).

zolpidem potentiation of I_{GABA} without altering flurazepam and zolpidem binding (Hanson and Czajkowski, 2008). In addition, unlike other BZD-site ligands, zolpidem appears to be able to adopt several favourable orientations in the BZD binding pocket (Hanson *et al.*, 2008). Thus, depending on its orientation, the zolpidem binding site movements that are transduced to the rest of the protein may differ.

In contrast, intrasubunit disulphide trapping γ_2 β-strand 9 (S202C) to the γ_2 pre-M1 region (S230C) significantly enhanced both flurazepam and zolpidem potentiation of I_{GABA} (Figures 5 and 9, Table 1), indicating that tethering β-strand 9 to the pre-M1 region (β-strand 10) traps the receptor in a more favourable conformation for BZD positive modulation. In related glycine receptors, Zn^{2+} binding to a site between β-strand 9 and β-strand 10 enhances receptor function supporting the idea that tethering β-strand 9 to β-strand 10 stabilizes the protein in a conformation that favours activation (Miller *et al.*, 2005). Intersubunit disulphide bonds formed at the α/γ coupling interface between α_1Loop 2 and γ_2Loop 9 (α_1D56C/γ_2L198C) prevent flurazepam and zolpidem from efficiently modulating I_{GABA} (Figures 7 and 9). Based on these data, we speculate that binding of BZD-site agonists destabilizes intersubunit interactions at the α/γ subunit coupling interface allowing movement of γ_2 β-strand 9 towards β-strand 10 and the pre-M1 region.

As none of the above disulphide bonds affected negative modulation of I_{GABA} by DMCM (Figures 4,5,7, and S2), rearrangements in the α_1/γ_2 coupling interface are likely not to be responsible for the actions of negative BZD modulators. This is consistent with our previous findings that residues in the γ_2 pre-M1 region and M2-M3 loop, which are required for BZD potentiation of $I_{GABA,}$ are not critical for inhibition of I_{GABA} by DMCM (Boileau and Czajkowski, 1999), and that only positive BZD modulators induce structural rearrangements in the γ_2Loop 9 region near the coupling interface (Hanson and Czajkowski, 2008).

Changes in maximal BZD potentiation of I_{GABA} can arise via several mechanisms, including alterations in BZD binding, changes in coupling BZD binding to potentiation, and/or shifts in GABA EC_{50}. While we cannot completely rule out effects on BZD binding, we believe that the effects are likely not due to changes in BZD binding. In previous studies, we demonstrated that residues in the γ_2Loop 9 region are not involved in BZD binding using radioligand binding assays (Hanson and Czajkowski, 2008; Hanson *et al.*, 2008). In addition, the mutations are located at the coupling interface and are not near the BZD binding site (Figure 1). Moreover, because our experiments were done at saturating concentrations of BZD, the data demonstrate that the mutations alter efficient coupling of BZD binding to modulation of I_{GABA} (BZD efficacy). The increases in flurazepam and zolpidem potentiation for γ_2S202C/S230C are also not due to changes in GABA dose–response, because the mutation had no effect on GABA EC_{50} (Table 1). Some mutations caused small but significant changes in GABA EC_{50} raising the possibility that the changes in BZD potentiation observed are a consequence of GABA EC_{50} alterations. BZD positive modulators enhance $GABA_A$ receptor current by decreasing GABA EC_{50}, whereas negative modulators, like DMCM, inhibit $GABA_A$ receptor current by increasing GABA EC_{50}. Using a simple model, if a mutation and/or disulphide bond shifts the GABA dose–response curve to the left, one would predict that the perturbation would decrease both flurazepam and zolpidem potentiation and would enhance DMCM inhibition. Intrasubunit disulphide bonds between γ_2S187C/L206C and γ_2S195C/F203C decreased GABA EC_{50} (1.8- and 3.5-fold respectively). While we observed a significant decrease in flurazepam potentiation of I_{GABA} for both mutants, zolpidem and DMCM modulation were unchanged (Figure 4, Table 1) indicating that the shift in GABA EC_{50} was not responsible for the observed changes in flurazepam potentiation. The intersubunit disulphide bond between α_1Loop 2 and γ_2Loop 9 (α_1D56C/γ_2L198C) also decreased GABA EC_{50} (1.7-fold, Table 2). In this case, the disulphide bond decreased flurazepam and zolpidem potentiation but had no effect on DMCM inhibition, again suggesting that a simple shift in GABA EC_{50} is not responsible. In many cases, the mutations affects on GABA EC_{50} and BZD potentiation were not correlated; some mutations significantly altered BZD potentiation without affecting GABA EC_{50} whereas others affected GABA EC_{50} without changing BZD potentiation (Tables 1, 2, and S1). Together, these observations support the idea that the mutations and disulphide bonds formed in this region specifically affect coupling of BZD binding to positive modulation of I_{GABA} and that the α/γ interface is an important part of the transduction pathway for BZD potentiation. This is consistent with our previous data demonstrating that flurazepam and zolpidem significantly slowed covalent modification of γ_2R197C in Loop 9, whereas DMCM, GABA and the allosteric modulator pentobarbital had no effects (Hanson and Czajkowski, 2008), indicating that movements in this region are specific for positive BZD modulators.

GABA-induced channel activation requires movements at the α_1/γ_2 coupling interface

Disulphide trapping α_1Loop 2 (α_1D56C) to γ_2 β-strand 1 (γ_2P64C) significantly decreased maximal GABA-induced current (Figure 8). Changes in GABA I_{max} can be attributed to changes in GABA binding (k_{on}, k_{off}), channel gating (α or β), and/or single-channel conductance. At high saturating agonist concentrations, the maximal current activation rate is limited by the channel opening step or β. Thus, an increase in I_{max} following DTT treatment is consistent with changes in channel gating or channel conductance. Because the disulphide bond is only at a single-subunit interface and is localized away from the channel vestibule, a change in gating is the simplest explanation. Detailed kinetic analyses are required to quantitatively tease apart the effects of this mutation on microscopic binding affinity and channel gating properties. Nonetheless, the data indicate that although the γ_2 subunit does not directly participate in GABA binding, movements at the single α_1/γ_2 coupling interface are required for efficient coupling of GABA binding to channel activation. Comparison of the crystal structures of the related bacterial pentameric ligand-gated ion channels, ELIC and GLIC, in presumed closed and open channel conformations suggests that channel activation is accompanied by a rearrangement of loops in the coupling interfaces including a downward motion of Loop 2 and outward movements of the M2-M3 loop (Bocquet *et al.*, 2009; Hilf and Dutzler, 2009). Thus, tethering α_1Loop 2 to γ_2 β-strand 1 may prevent this downward motion of Loop 2, whereas tethering α_1Loop 2 to γ_2 Loop 9 (α_1D56C/γ_2L198C) does not. α_1D56C/γ_2P64C also decreased maximal flurazepam and zolpidem potentiation of I_{GABA} (Table 2) consistent with this region being involved in BZD positive modulator actions.

Summary and conclusions

In summary, the data in this study provide new insights into the transduction pathway for BZD allosteric modulation of the $GABA_A$ receptor. We found that mutations throughout the α/γ coupling interface reduce BZD potentiation of I_{GABA}, supporting the idea that this region is important for efficient coupling of BZD binding to modulation of I_{GABA}. We demonstrate that restricting local movements in the α/γ coupling interface through disulphide trapping specifically affects potentiation of I_{GABA} by BZD-site agonists and does not affect negative modulation by BZD inverse agonists, demonstrating that the allosteric pathways for positive and negative modulation of I_{GABA} by BZDs are different. Our data support a mechanism of BZD action in which coupling between BZD-site agonist binding and the potentiation of I_{GABA} occurs by movements of γ_2Loop 9, γ_2 β-strand 9, the γ_2 pre-M1 region and Loop 2 in the adjacent α_1 subunit (Figure 9).

Based on the crystal structures of ELIC and GLIC in presumed closed and open conformations (Bocquet *et al.*, 2009;

Hilf and Dutzler, 2009) as well as comparison of low-resolution nicotinic acetylcholine receptor structures with and without agonist (Unwin, 2005), channel activation appears to be accompanied by a reorganization of subunit–subunit interfaces. We envision that neurotransmitter binding destabilizes subunit–subunit interface interactions, which help maintain the resting/closed channel state, and that this may be a common mechanism underlying pentameric LGIC activation. In a related fashion, we speculate that the actions of allosteric drug modulators are also driven by realignments at subunit–subunit interfaces. While BZDs do not activate $GABA_A$ receptors directly, our data demonstrate that positive BZD-modulator binding at the α/γ interface induces rearrangements of the α/γ coupling interface. Moreover, our data suggest that constraining movement of the α/γ coupling interface inhibits GABA-induced channel activation. Thus, BZD-induced movements at the α/γ coupling interface are likely to synergize with the rearrangements induced by GABA binding at the β/α subunit interfaces to enhance channel activation by GABA.

Acknowledgements

We thank James Raspanti for technical assistance and preparation of oocytes. This work was supported by the National Institutes of Health NIH [Grant: F32 MH082504] to S.M.H and [Grant: NS34727] to C.C.

Conflicts of interest

None to declare.

References

Akabas MH (2004). GABAA receptor structure-function studies: a reexamination in light of new acetylcholine receptor structures. Int Rev Neurobiol 62: 1–43.

Alexander SP, Mathie A, Peters JA (2009). Guide to Receptors and Channels (GRAC). 4th edn. Br J Pharmacol 158 (Suppl. 1): S1–254.

Bali M, Jansen M, Akabas MH (2009). GABA-induced intersubunit conformational movement in the GABAA receptor alpha 1M1-beta 2M3 transmembrane subunit interface: experimental basis for homology modeling of an intravenous anesthetic binding site. J Neurosci 29: 3083–3092.

Bass RB, Butler SL, Chervitz SA, Gloor SL, Falke JJ (2007). Use of site-directed cysteine and disulfide chemistry to probe protein structure and dynamics: applications to soluble and transmembrane receptors of bacterial chemotaxis. Methods Enzymol 423: 25–51.

Baumann SW, Baur R, Sigel E (2002). Forced subunit assembly in alpha1beta2gamma2 GABAA receptors. Insight into the absolute arrangement. J Biol Chem 277: 46020–46025.

Bera AK, Akabas MH (2005). Spontaneous thermal motion of the GABA(A) receptor M2 channel-lining segments. J Biol Chem 280: 35506–35512.

Boileau AJ, Czajkowski C (1999). Identification of transduction elements for benzodiazepine modulation of the GABA(A) receptor: three residues are required for allosteric coupling. J Neurosci 19: 10213–10220.

Boileau AJ, Kucken AM, Evers AR, Czajkowski C (1998). Molecular dissection of benzodiazepine binding and allosteric coupling using chimeric gamma-aminobutyric acidA receptor subunits. Mol Pharmacology 53: 295–303.

Boileau AJ, Baur R, Sharkey LM, Sigel E, Czajkowski C (2002). The relative amount of cRNA coding for gamma2 subunits affects stimulation by benzodiazepines in GABA(A) receptors expressed in Xenopus oocytes. Neuropharmacology 43: 695–700.

Bocquet N, Nury H, Baaden M, Le Poupon C, Changeux JP, Delarue M *et al.* (2009). X-ray structure of a pentameric ligand-gated ion channel in an apparently open conformation. Nature 457: 111–114.

Brejc K, van Dijk WJ, Klaassen RV, Schuurmans M, van Der Oost J, Smit AB *et al.* (2001). Crystal structure of an ACh-binding protein reveals the ligand-binding domain of nicotinic receptors. Nature 411: 269–276.

Campo-Soria C, Chang Y, Weiss DS (2006). Mechanism of action of benzodiazepines on GABAA receptors. Br J Pharmacol 148: 984–990.

Careaga CL, Falke JJ (1992). Structure and dynamics of Escherichia coli chemosensory receptors. Engineered sulfhydryl studies. Biophys J 62: 209–216. discussion 217-209.

Downing SS, Lee YT, Farb DH, Gibbs TT (2005). Benzodiazepine modulation of partial agonist efficacy and spontaneously active GABA(A) receptors supports an allosteric model of modulation. Br J Pharmacol 145: 894–906.

Eghbali M, Curmi JP, Birnir B, Gage PW (1997). Hippocampal GABA(A) channel conductance increased by diazepam. Nature 388: 71–75.

Hanson SM, Czajkowski C (2008). Structural mechanisms underlying benzodiazepine modulation of the GABA(A) receptor. J Neurosci 28: 3490–3499.

Hanson SM, Morlock EV, Satyshur KA, Czajkowski C (2008). Structural requirements for eszopiclone and zolpidem binding to the gamma-aminobutyric acid type-A (GABAA) receptor are different. J Med Chem 51: 7243–7252.

Hilf RJ, Dutzler R (2009). Structure of a potentially open state of a proton-activated pentameric ligand-gated ion channel. Nature 457: 115–118.

Horenstein J, Wagner DA, Czajkowski C, Akabas MH (2001). Protein mobility and GABA-induced conformational changes in GABA(A) receptor pore-lining M2 segment. Nat Neurosci 4: 477–485.

Horenstein J, Riegelhaupt P, Akabas MH (2005). Differential protein mobility of the gamma-aminobutyric acid, type A, receptor alpha and beta subunit channel-lining segments. J Biol Chem 280: 1573–1581.

Jansen M, Akabas MH (2006). State-dependent cross-linking of the M2 and M3 segments: functional basis for the alignment of GABAA and acetylcholine receptor M3 segments. J Neurosci 26: 4492–4499.

Karlin A, Akabas MH (1998). Substituted-cysteine accessibility method. Methods Enzymol 293: 123–145.

Kosolapov A, Deutsch C (2003). Folding of the voltage-gated K+ channel T1 recognition domain. J Biol Chem 278: 4305–4313.

Lavoie AM, Twyman RE (1996). Direct evidence for diazepam modulation of GABAA receptor microscopic affinity. Neuropharmacology 35: 1383–1392.

Lu J, Deutsch C (2001). Pegylation: a method for assessing topological accessibilities in Kv1.3. Biochemistry 40: 13288–13301.

Mellor JR, Randall AD (1997). Frequency-dependent actions of benzodiazepines on GABAA receptors in cultured murine cerebellar granule cells. J Physiol 503 (Pt 2): 353–369.

Mercado J, Czajkowski C (2006). Charged residues in the alpha1 and beta2 pre-M1 regions involved in GABAA receptor activation. J Neurosci 26: 2031–2040.

Miller PS, Da Silva HM, Smart TG (2005). Molecular basis for zinc potentiation at strychnine-sensitive glycine receptors. J Biol Chem 280: 37877–37884.

Miyazawa A, Fujiyoshi Y, Unwin N (2003). Structure and gating mechanism of the acetylcholine receptor pore. Nature 423: 949–955.

Negroiu G, Dwek RA, Petrescu SM (2000). Folding and maturation of tyrosinase-related protein-1 are regulated by the post-translational formation of disulfide bonds and by N-glycan processing. J Biol Chem 275: 32200–32207.

Rogers CJ, Twyman RE, Macdonald RL (1994). Benzodiazepine and beta-carboline regulation of single GABAA receptor channels of mouse spinal neurones in culture. J Physiol 475: 69–82.

Rosen A, Bali M, Horenstein J, Akabas MH (2007). Channel Opening by Anesthetics and GABA Induces Similar Changes in the GABAA Receptor M2 Segment. Biophys J 92: 3130–3139.

Rusch D, Forman SA (2005). Classic benzodiazepines modulate the open-close equilibrium in alpha1beta2gamma2L gamma-aminobutyric acid type A receptors. Anesthesiology 102: 783–792.

Shelness GS, Thornburg JT (1996). Role of intramolecular disulfide bond formation in the assembly and secretion of apolipoprotein B-100-containing lipoproteins. J Lipid Res 37: 408–419.

Sigel E (2002). Mapping of the benzodiazepine recognition site on GABA(A) receptors. Curr Top Med Chem 2: 833–839.

Sine SM, Engel AG (2006). Recent advances in Cys-loop receptor structure and function. Nature 440: 448–455.

Unwin N (2005). Refined structure of the nicotinic acetylcholine receptor at 4A resolution. J Mol Biol 346: 967–989.

Venkatachalan SP, Bushman JD, Mercado JL, Sancar F, Christopherson KR, Boileau AJ (2007). Optimized expression vector for ion channel studies in Xenopus oocytes and mammalian cells using alfalfa mosaic virus. Pflugers Arch 454: 155–163.

Xu M, Akabas MH (1996). Identification of channel-lining residues in the M2 membrane-spanning segment of the GABA(A) receptor alpha1 subunit. J Gen Physiol 107: 195–205.

Yang Z, Webb TI, Lynch JW (2007). Closed-state cross-linking of adjacent beta1 subunits in alpha1beta1 GABAa receptors via introduced 6′ cysteines. J Biol Chem 282: 16803–16810.

Supporting information

Additional Supporting Information may be found in the online version of this article:

Figure S1 DTT does not significantly affect FZM potentiation of double cysteine mutants. Changes in FZM potentiation following treatment with DTT is graphed for WT and mutant receptors. The effect of DTT treatment was calculated as: [((FZM potentiation$_{after}$ /FZM potentiation$_{before}$) − 1) × 100]. Note that DTT treatment did not significantly change FZM potentiation for the mutant receptors compared to WT receptors.

Figure S2 DMCM modulation of WT and mutant $GABA_A$ receptors. Maximal inhibition of GABA EC_5 responses by DMCM (1 μM) is graphed for WT and mutant receptors. Inhibition of GABA current was calculated as [($I_{GABA+DMCM}/I_{GABA}$) − 1]. DMCM inhibition for the mutant receptors was not significantly different from WT.

Figure S3 FZM potentiation of I_{GABA} is significantly affected by mutations in the α_1/γ_2 coupling interface. *Left panels (A,D,F)*, Models of the $GABA_AR$ α_1 (red) and γ_2 (blue) subunit coupling interface are shown. Loops and β-strands are coloured as in Figure 1: γ_2Loop 9, purple; γ_2 β-strand 9, orange; $\gamma_2$pre-M1, yellow; γ_2Loop 7, red; α_1Loop2, green; α_1Loop7, blue. Residues mutated to cysteine are shown in stick representation except in panel (A) where only every other Loop 9 residue is shown for clarity. *Right panels (B,C,E,G)*, Potentiation of GABA EC_5 current by 10 μM FZM is graphed for WT (×), single-cysteine mutant receptors (•), and double cysteine mutant receptors (○). A dashed line indicates the level of potentiation for the single α_1 subunit cysteine mutant that is expressed with multiple γ_2 mutant subunits. Data represent mean ± SD from at least three separate experiments. (**P<0.01), FZM potentiation of the double cysteine mutant receptor was significantly reduced compared to both single-cysteine mutants. Potentiation values were calculated as [($I_{GABA+FZM}/I_{GABA}$) − 1] and are reported in Table S1.

Table S1 Summary of GABA, flurazepam, and zolpidem data from WT and α_1/γ_2 cysteine mutant receptors used for *inter*-subunit disulphide bonds.

Please note: Wiley-Blackwell are not responsible for the content or functionality of any supporting materials supplied by the authors. Any queries (other than missing material) should be directed to the corresponding author for the article.